

Quantum computation by coupled quantum dot system and controlled NOT operation

Tetsufumi Tanamoto

Research and Development Center, Toshiba Corporation, Saiwai-ku, Kawasaki 210-8582, Japan

(February 5, 2020)

A quantum computer based on an asymmetric coupled dot system has been proposed and shown to operate as the controlled NOT gate. The basic idea is (1) the electron is localized in one of the asymmetric coupled dots. (2) The electron transfer takes place from one dot to the other when the energy-levels of the coupled dots are set close. (3) The Coulomb interaction between the coupled dots mutually affects the energy levels of the other coupled dots. The proposed system can be realized by developing the technology of the single electron memory using Si nanocrystals and the direct combination of the quantum circuit and the conventional circuit is possible.

Since Shor's factorization program was proposed, many studies have been carried out with a view to realizing the quantum computer [1–6]. Although coherence is necessary for a quantum calculation, it is considered to be difficult to maintain coherence in the entire calculation process throughout the entire circuit. Thus, it will be more efficient and more realistic to combine the quantum computational circuit and the conventional LSI circuit in the same chip. Some proposals regarding the quantum computer based on semiconductor physics have been made from this viewpoint [3–6].

Kane [6] proposed the Si-based quantum dot computer using NMR of dopants (phosphorus). This idea is very promising because the qubits are isolated from the external environment which causes decoherence. But controlling the implantation of phosphorus into the definite position of the Si substrate will be difficult even with the future technology and the usage of the magnetic field seems to be undesirable in the conventional Si LSI circuit. Here we propose a coupled quantum dot system of a quantum computer which can be operated only by electrical effects and show that it can operate as a controlled NOT gate. It is shown to be realized by developing the technology of a single electron memory of Si nanocrystals [7,8].

The controlled NOT operation is given by [3]: $|\epsilon_1\rangle|\epsilon_2\rangle \rightarrow |\epsilon_1\rangle|\epsilon_1 \oplus \epsilon_2\rangle$ (modulo 2) where ϵ_1 shows a *control qubit* and ϵ_2 shows a *target qubit*. The value of ϵ_1 remains unchanged whereas that of ϵ_2 is changed only if $\epsilon_1 = 1$. This operation is important because it acts as a measurement gate and produces the entanglement [3] which plays an important role in quantum cryptography gates [9].

Coupled quantum dot systems with a few electrons have been extensively investigated in regard to many-body effects such as Coulomb blockade [10–15]. From the experiments by van der Vaart [12], we can see that

the electron transfer between dots occurs when the discrete energy-level of one of the dots matches that of the other dot of the coupled dots. Pfannkuche *et al.* [13] showed theoretically that, as the result of the correlations between a few electrons in quantum dots, the electrons behave as if they were noninteracting electrons. Crouch *et al.* [14,15] showed that, if the tunneling barrier is low and the coupling of the two dots is strong, the coupled dots behave as a large single dot in Coulomb blockade phenomenon. This means that, if the tunneling barrier between the dots is small enough, it is possible that only one electron exists in the coupled dots.

Thus, we can consider the electronic state of the two coupled dots in the range of the free electron approximation [16,17] at the first step of investigation. When two dots of different size are coupled and one excess electron is inserted, the energy-levels of the total coupled dot system show the localized state of wave function reflecting the different energy-levels of the independent isolated dots [16]. When gate bias voltage is applied and the potential slope is changed, there appears a gate bias voltage, V_{res} , at which the two energy-levels of the original single dots coincide and the electron transfers to another dot (resonant tunneling). Coupling removes the degeneracy of energy-levels in the single dot quantum states, and produces new states of delocalization such that the even-parity and odd-parity wave functions spread over the two coupled dots. Thus, if we regard the perfect localization of the charge in one of the coupled dots as $|1\rangle$ state and that in the other dot as $|0\rangle$ state, we can constitute *qubit* by the coupled quantum dots (Fig. 1).

The point is, by adjusting the gate bias, we can control the electronic state from the localized regions ($|1\rangle$ and $|0\rangle$) to the intermediate delocalized region only where the electron transfers from one dot to the other in the coupled dots in a short time (\sim pico second) [16,17]. As the tunneling barrier structure is asymmetric, the leak current through the coupled dot system is extremely small [18] and neglected actually.

When we array the above coupled dots (qubits) side by side, the charge distribution of the electron in a qubit changes the potential profiles and the energy-levels of the neighboring qubits by its electric field. We assume that the electron transfer between different qubits can be neglected. Then the electronic state in a qubit is affected by whether the electrons in other qubits stay in the $|1\rangle$ state, $|0\rangle$ state or arbitrary superposition state of $|1\rangle$ and $|0\rangle$. By changing the charge distribution of the array of qubits, we can operate the total charge distribution of the electrons and the quantum circuit. Figure 2 shows

the case of the two-qubit controlled NOT gate where one set of the coupled dots operates as a *control qubit* and the other as a *target qubit*. We numerically show this array of the coupled quantum dot operates as the controlled NOT gate later.

One of the candidates of the coupled dots of quantum computer is considered to be the Si nanocrystals embedded in the gate insulator (Fig.3). This is based on the similar technology of Si LSI as Tiwari's single electron memory [7,8] which is extensively investigated because it operates at room temperature. The excess charge is supplied from the inversion layer in the substrate. By setting larger dots near the channel, the structure shown in Fig. 2 can be realized. The arrangement of the gate electrodes which control the individual qubits depends on the individual algorithm. The simplest form is the case where there are two gate electrodes and two sets of coupled dots (Fig. 2), which works as the controlled NOT gate explained in this paper. The *measurements* process is operated by the upper gate electrode which controls the overall channel carrier density. The upper gate also protects the electronic states in the dots from disturbance by shielding the external electromagnetic field. The qubits interact mutually and the distribution of the charges affects the current flow (channel conductance) between the source and drain and the threshold gate voltage. A $|11\rangle$ state shifts the threshold voltage most and a $|00\rangle$ state shifts it least. Because of the sloping channel depth from the source to the drain, the $|10\rangle$ state and $|01\rangle$ state can be distinguished. Thus the quantum mechanical calculation proceeds as follows: (0)To *initialize* the charge distribution (initial quantum states), a large voltage is applied on the upper gate over the coupled dots, and unifies the charge distribution in the coupled dots, (1)The input and output signals are added through the gates over each qubit, (2)the final distribution of charges (final quantum states) are detected by the current between the source and drain and the threshold voltage shifts of the upper gates over the coupled dot system.

This structure of the proposed system has the merit that the charge distribution in the coupled dot system, which is considered to be a very small signal, is expected to be detected by the channel conductance with high sensitivity like the single electron memory [7].

Similar to Tiwari's single electron memory, the charging effect appears between the coupled dots and the channel region and the probability that two electrons come into the qubits is very small as long as the capacitance of the junction is sufficiently small.

Decoherence of the transport in Si nanocrystals is considered to be caused by the interface trap states [19,20]. However, because the proposed quantum computer is expected to be embedded as a part of the conventional Si MOSFET circuit, the problem of decoherence can be ameliorated by the advancing cleanness technology of Si interface.

Bellow, we show the static properties of the wave function of the localized electron by using the S-matrix theory

and the controlled NOT operation of the coupled dots. The periodical motion of the localized electron is shown by solving a time-dependent Schrödinger equation.

The static properties of the wave function in the coupled dots can be shown by applying the S-matrix theory [21] to the one-dimensional case. One-dimensional Schrödinger equation is given:

$$\left[-\frac{\hbar^2}{2m_i} \frac{\partial^2}{\partial z^2} + V_i(z)\right]\psi_i(z) = E\psi_i(z) \quad (1)$$

where $i(= 1, \dots, N_m)$ show the number of the mesh in the calculation. It is well known that a relatively small number of N_m is sufficient for the calculation (here $N_m \sim 1000$). The electric fields by other coupled dots are considered to be included in the potential, $V_i(z)$. We use the plane wave approximation for the wave functions:

$$\psi_i(x) = A_i e^{ik_i x} + B_i e^{-ik_i x} \quad (2)$$

The boundary conditions are given

$$\psi_i(x) = \psi_{i+1}(x), \quad \frac{1}{m_i} \frac{\partial \psi_i}{\partial x} = \frac{1}{m_{i+1}} \frac{\partial \psi_{i+1}}{\partial x} \quad (3)$$

which determines the coefficient A_i, B_i :

$$\begin{bmatrix} A_{i+1} \\ B_{i+1} \end{bmatrix} = \begin{bmatrix} (1+r_i)e^{ik_i x} & (1-r_i)e^{-ik_i x} \\ (1-r_i)e^{ik_i x} & (1+r_i)e^{-ik_i x} \end{bmatrix} \begin{bmatrix} A_i \\ B_i \end{bmatrix} \quad (4)$$

where $r_i = (k_i/m_i^*)/(k_{i+1}/m_{i+1}^*)$. Here we assume that the electron is inserted from the channel layer ($i = 0$ part) and neglect the reflection amplitude of the wave function of the gate electrode ($B_{N_m} = 0$), similar to Ref. [21]. Then the transmission coefficient is given:

$$T_{N_m}(E) \equiv \frac{|k_{N_m}|}{|k_0|} |A_{N_m}|^2. \quad (5)$$

Discrete energy-levels of the coupled dots are those when this transmission coefficient has a maximum. We can estimate the effects of the Coulomb interaction of the control qubit on the target qubit shown in Fig. 2. The Coulomb interaction on the dot a_1 from the dot a_2 , and that from the dot b_2 are given by $U_{a_1 a_2} = e^2/\epsilon r_{a_1 a_2} \rho_{a_2}$, $U_{a_1 b_2} = e^2/\epsilon r_{a_1 b_2} \rho_{b_2}$, respectively, where ρ_i is the density of the wave function of dot i and r_{ij} shows the distance between the center of the dot i and j . We set $\rho_i = 0$ or 1 depending on the existence of the localized electron of the neighboring qubits. The Coulomb interaction on the dot b_1 is treated similarly. These Coulomb interactions are added to the potential bottom of the target qubit. For simplicity, we neglect the self-consistent effects.

The localized electron in one of the coupled dots moves into the other dot only if the two discrete energy-levels are set close (on resonance). The slight change of the relative energy-level by the electric field generated by the other set of coupled dots makes impossible the transfer of the localized electron from one dot to the other. The

basic concept of this scheme is similar to that of Barenco *et al.* [3]. Whereas Barenco *et al.* uses the ground state and excited state in a single dot with optical resonant effects, we are using only the ground state of the coupled dots only with electrical resonant effects (*ground state operation*). The smaller the size of the dot, the more stable is the operation.

Figures 4 and 5 show the calculated results of the controlled NOT operation in Si/SiO₂ ($\epsilon = 4$) material. The barrier height of SiO₂ is assumed to be 3.1 eV and the effective mass of Si and SiO₂ are assumed to be $0.2m_0$ where m_0 is a mass of free electron. As the tunneling barrier is sufficiently high, the coupled dot system can be made smaller in Si/SiO₂ system than in GaAs/AlGaAs system [22]. The diameter of the larger quantum dot is 6nm and that of the smaller is 4nm where the thickness of the tunneling barrier is 1.4nm. The distance between centers of the dots of the same size is assumed to be 20nm (4×10^{12} dots/cm²). These values are taken from the experiments by Tiwari *et al.* [7]. The thinner tunneling barrier between the dots in a qubit becomes (≤ 1 nm), the weaker the rate of the localization effect is.

Electron in a target qubit is localized in a larger dot at lower gate bias region (region A⁽¹⁾) in the case where control qubit is in $|1\rangle$ state in Fig.4). As the gate voltage is applied, the energy-level of the localization in the larger dot exceeds that of the smaller dot. At $V_G = V_{\text{res}}^{(1)}$ (center of the left hatched region in Fig.4), the wave function of the lowest energy state (even-parity) and that of the excited state (odd-parity) spread over the two dots with equal weight, when the control qubit is in $|1\rangle$ state. The degenerate energy-levels of the single dots split by the coupling of the dots and show the small energy difference, ΔE ($\sim 6.28 \times 10^{-5}$ eV: which is not distinguishable in the figure). This resonant gate bias shifts toward the higher bias region in the case where the control bit is in $|0\rangle$ state. This is because the electron in the control qubit is localized in a smaller dot and the band bottom of the smaller dot in the target qubit is raised (Fig.5(b)). Thus, when we apply the voltage, $V_{\text{res}}^{(1)}$, in a half time of the oscillation with time period, $\tau_s \sim \hbar/2\Delta E$ (~ 5.2 pico sec), the electron moves between alternate dots only if the control qubit is in $|1\rangle$ state and we can show the controlled NOT operation in the coupled quantum dot system.

Note that the wave function shown in Fig.4 is the static one and dynamical properties can be easily discussed by solving the time-dependent Schrödinger equation [17] as follows. The localized wave functions in a quantum dot a and b and the eigenenergies are expressed as $\psi_a(x)$ and $\psi_b(x)$, and, E_a and E_b , respectively, which are assumed to be far apart from each other. Then the coupled wave function is constituted by these wave functions as,

$$\psi(x, t) = a(t)\psi_a(x) + b(t)\psi_b(x). \quad (6)$$

The Hamiltonian of the Schrödinger equation, $i\hbar\partial\psi/\partial t = H\psi$, is given by

$$H = -\frac{\hbar^2}{2m} \frac{\partial^2}{\partial x^2} + V_a(x) + V_b(x) - V_0, \quad (7)$$

where $V_0 (= 3.1 \text{ eV})$ is a barrier height between the quantum dot a and b . This equation is easily solved and the eigenenergies are given as

$$\omega_{\pm} = (\omega_a + \omega_b)/2 \pm \omega_0 \quad (8)$$

where $\omega_a = E_a/\hbar$, $\omega_b = E_b/\hbar$, $c_a = \langle 1|V_a - V_0|2\rangle/\hbar$, $c_b = \langle 2|V_b - V_0|2\rangle/\hbar$ and $\omega_0 = \sqrt{[(\omega_a - \omega_b)/2]^2 + c_a c_b}$. In particular, when the applied bias puts the energy-level of dot a and dot b at the same level ($\omega_a = \omega_b$), and the charge is localized in one of the coupled dots in the initial state ($a(0) = 1, b(0) = 0$), we have:

$$a(t) = e^{-i\omega_a t} \cos \omega_0 t, \quad b(t) = -i e^{-i\omega_a t} \frac{c_b}{\omega_0} \sin \omega_0 t. \quad (9)$$

This shows that the localized electron moves completely between dot a and dot b with a period, $\pi/(2\omega_0)$. Thus we can show the charge transfer is realized when we apply the voltage at which the energy-levels of the initially isolated dot coincide, which also corresponds to the case where the energy-level of ground state and that of the excited state of the coupled dots approach most closely (hatched area in Fig.4), in the time period of $\pi/(2\omega_0)$. Moreover, in the case of different initial condition of charge distribution, ($|0\rangle + |1\rangle$) / $\sqrt{2}$ is realized as a static state.

Time spent for the transfer of the charge in a coupled quantum dot is given as $\tau_d = \pi/\omega_0$ with:

$$\omega_0 = \frac{4}{\hbar} \left(\frac{V_0 - E}{V_0} \right) \frac{E}{1 + Kl_w} e^{-Kl_d} \quad (10)$$

where l_w is an average width of the quantum dot ($= 5$ nm), l_d ($= 1.4$ nm) is the width of the tunneling barrier between the two dots, $K = \sqrt{2m(V_0 - E)/\hbar^2}$ and E is the energy of incident electron. We obtained $\tau_d \sim 23$ pico sec in the case of Fig.4, which is longer than the time obtained above (τ_s). This is because this time-dependent approach numerically identifies the exact results when the two dots are far apart [16]. In any event, this numerical mismatch never changes the physical aspects of the coupled dot system.

The coupled dots (qubits) can be fabricated by applying the self-limiting oxidation process of Si nanostructure [23]. For example, the oxidation process after forming Si nanocrystals on a thin amorphous Si layer via SiO₂ thin film changes the amorphous Si layer and leaves Si dots only under the top Si nanocrystals which also remain. Thus forming the coupled dot system is more feasible than controlling donor atoms in substrates. The small fluctuation of the dot sizes is not serious because the on/off gate voltage can be adjusted to be initialized depending on each energy-level of each qubit. The effects of phonons are expected to be reduced in quantum dots and the phase coherence is improved [19]. Another

concern is that interface traps may be another localized state and break coherence of the quantum calculation. However, the density of the trap state ($\sim 10^{10} \text{ cm}^{-2}$) is smaller than the assembly of the nanocrystals ($\sim 10^{12} \text{ cm}^{-2}$). Although the other effects such as noises generated by the gate voltage fluctuations might lead to the decoherence, the proposed computational operations are based on the fundamental quantum effects about which a myriad of experiments have been done and shown their operations at least at low temperature. In any events, these problems will hopefully be ameliorated as the process technology of conventional LSI advances.

In conclusion, we have proposed a quantum computer based on the coupled dot system, which can be realized by developing the technology of the single electron memory with S nanocrystals. The basic idea is (1) the electron is localized in one of the asymmetric coupled dots. (2) The electron transfer takes place from one dot to the other when the energy-levels of the coupled dots are set close. (3) The Coulomb interaction between the coupled dots mutually affects the energy levels of the other coupled dots. The proposed system, where the direct combination of the quantum circuit and the conventional circuit is possible, is shown to be a promising candidate of the quantum computer.

[1] A. Ekert and R. Jozsa, *Rev. Mod. Phys.*, **68**, 733 (1996).
[2] N. A. Gershenfeld and I. L. Chaung, *Science*, **275**, 350 (1997).
[3] A. Barenco, D. Deutsch, A. Ekert, *Phys. Rev. Lett.*, **74**, 4083 (1995).
[4] D. Loss and D. P. Divincenzo, *Phys. Rev. A.*, **57**, 120 (1998).
[5] G. Burkard, D. Loss and D. P. Divincenzo, *cond-mat/9808026*.
[6] B. E. Kane, *Nature*, **393**, 133 (1998).
[7] S. Tiwari *et al.*, *Appl. Phys. Lett.*, **68**, 1377 (1996).
[8] L. Guo, E. Leobandung, S. Y. Chou, *Science*, **275**, 649 (1997).
[9] C. H. Bennett *et al.*, *Phys. Rev. Lett.*, **29** 1895 (1993).
[10] C. A. Stafford and S. Das Sarma, *ibid.*, **72**, 3590 (1994).
[11] J. Weiss, R. J. Haug, K. v. Klitzing, K. Ploog, *ibid.*, **71**, 4019 (1993).
[12] N.C. van der Vaart, S. F. Godijn, Y. V. Nazarov, C. J. P. M. Harmans, J. E. Mooij, *ibid.*, **74**, 4702 (1995).
[13] D. Pfannkuche and S. E. Ulloa, *ibid.*, **74**, 1194 (1995).
[14] C. H. Crouch, C. Livermore, R. M. Westervell, K. L. Campman, A. C. Gossard, *Appl. Phys. Lett.*, **71**, 817 (1997).
[15] F. R. Waugh *et al.*, *Phys. Rev. Lett.*, **75**, 705 (1995).
[16] A. Yariv, C. Lindsey, U. Sivan, *J. Appl. Phys.*, **58**, 366 (1985).
[17] N. Tsukada, A. D. Wieck, K. Ploog *Appl. Phys. Lett.*, **56**, 2527 (1990).

[18] B. Ricco and M. Y. Azbel, *Phys. Rev. B*, **29**, 1970 (1984).
[19] R. Tsu, *Physica B*, **189**, 235 (1993).
[20] Q. Ye, R. Tsu and E. H. Niccolian, *Phys. Rev. B*, **44**, 1806 (1991).
[21] R. Tsu and L. Esaki *Appl. Phys. Lett.*, **22**, 562 (1973).
[22] R. Tsu, *Nature*, **364**, 19 (1993).
[23] H. I. Liu, D. K. Biegelsen, F. A. Ponce, N. M. Johnson, R. F. W. Pease, *Appl. Phys. Lett.*, **64**, 1383 (1994).

ACKNOWLEDGMENTS

The author is grateful to K. Sato, S. Fujita, K. Ichimura and R. Ohba for fruitful discussion.

FIG. 1. Coupled quantum dot as qubit: large quantum dot and small quantum dot are coupled such that the larger dot is set close to the channel from where one excess electron is inserted into the coupled dots. The smaller dot is set near the gate electrode via thick tunnel barrier which controls the energy-levels of the coupled dots. The localized electron in a larger dot expresses the $|1\rangle$ state and that in a smaller dot expresses the $|0\rangle$ state.

FIG. 2. Quantum gates (controlled NOT gate) are constituted by setting the coupled dots of Fig.1 close to each other with the common channel. Solid lines show the path of electron tunneling. Dotted lines show the electric fields generated between quantum dots or between quantum dots and gates.

FIG. 3. An example of the N coupled dot system of quantum computing. Dots are coupled in the longitudinal direction. The electron transfer in the lateral direction is assumed to be neglected. The FET channel structure enables the detection of the small signal of the charge distribution in coupled quantum dots.

FIG. 4. Relation between the energy-levels of electrons of a target qubit and the gate bias for the cases in which the control qubit is in $|1\rangle$ state and $|0\rangle$ state. The structure is, channel/SiO₂(2.5nm)/Si nanocrystals (6nm:dot a)/SiO₂(1.4nm)/ Si nanocrystals (4nm:dot b)/SiO₂(7nm)/Gate. $A^{(1)}$ and $B^{(1)}$ show the localized regions in gate bias for a larger dot (dot a_1 in Fig.2) and a smaller dot (dot b_1 in Fig.2), respectively, when the control qubit is in $|1\rangle$ state. $A^{(0)}$ and $B^{(0)}$ show similar regions when the control qubit is in $|0\rangle$ state. Hatched areas show the regions of the delocalization where the wave functions spread over the two dots. This area shifts depending on whether the control qubit is in $|1\rangle$ state or $|0\rangle$ state. At the boundaries of these areas, wave functions are delocalized less than 98 % in one of the dots and at their centers, $V_{\text{res}}^{(1)}$ or $V_{\text{res}}^{(0)}$, wave functions are equally distributed in both dots.

FIG. 5. Spatial dependence of $|\psi|^2$ of the target qubit when the gate bias is $V_{\text{res}}^{(1)}$: (a) the control qubit is in $|1\rangle$ state (the charge of the control qubit is localized in a larger dot near the channel and the potential of the dot near the channel in target qubit is raised), (b) the control qubit is in $|0\rangle$ state (the charge of the control qubit is localized in a smaller dot and the potential of the smaller dot in target qubit is raised). Wave functions are normalized in the lateral regions of the figures. This shows the controlled NOT operation in which the state of the target qubit is changed in a few pico second (dynamical properties) only if the control qubit is in $|1\rangle$ state.

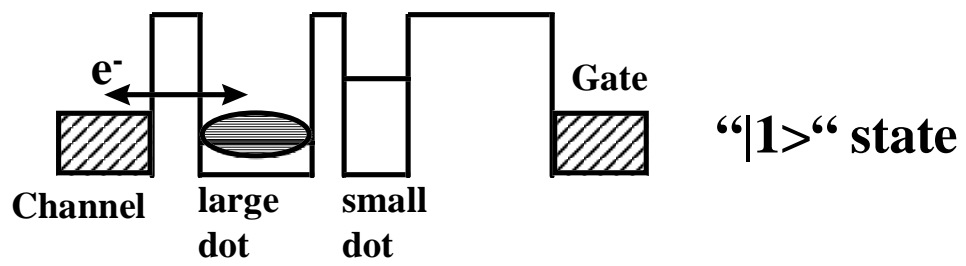


Fig. 1(a) : T.Tanamoto

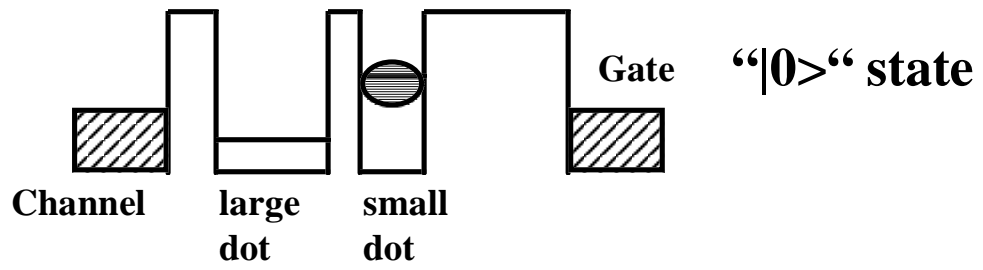


Fig. 1(b) : T.Tanamoto

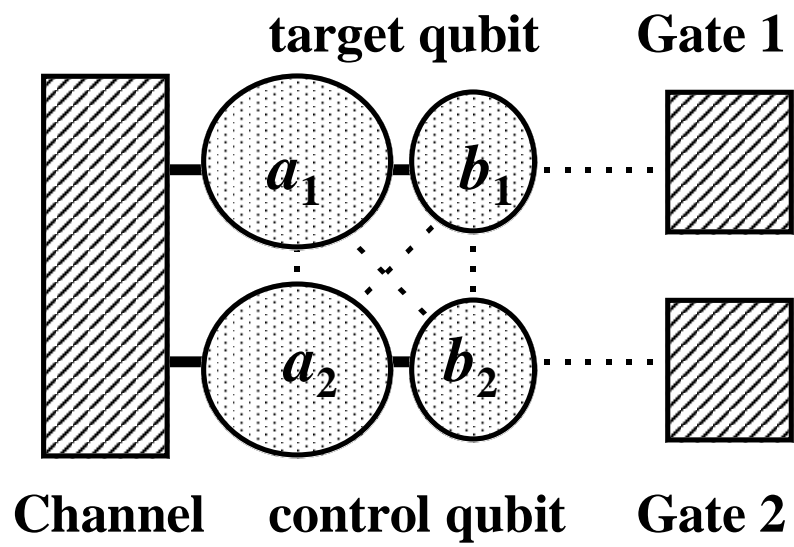


Fig. 2: T.Tanamoto

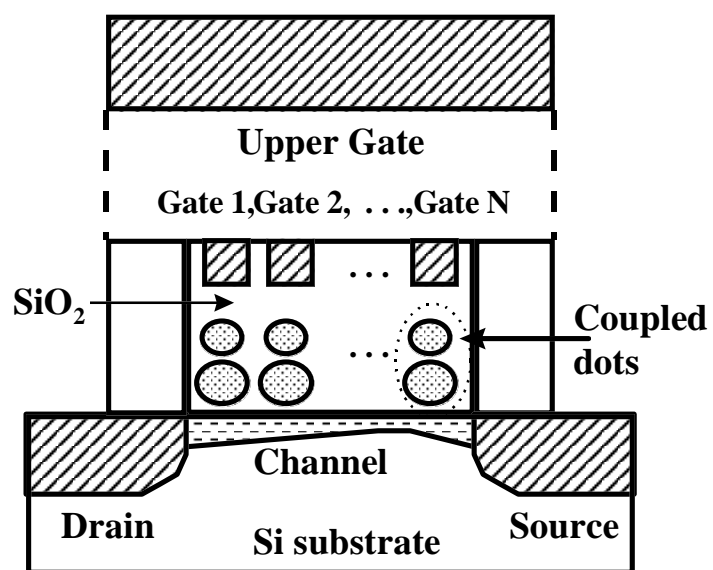


Fig. 3: T.Tanamoto

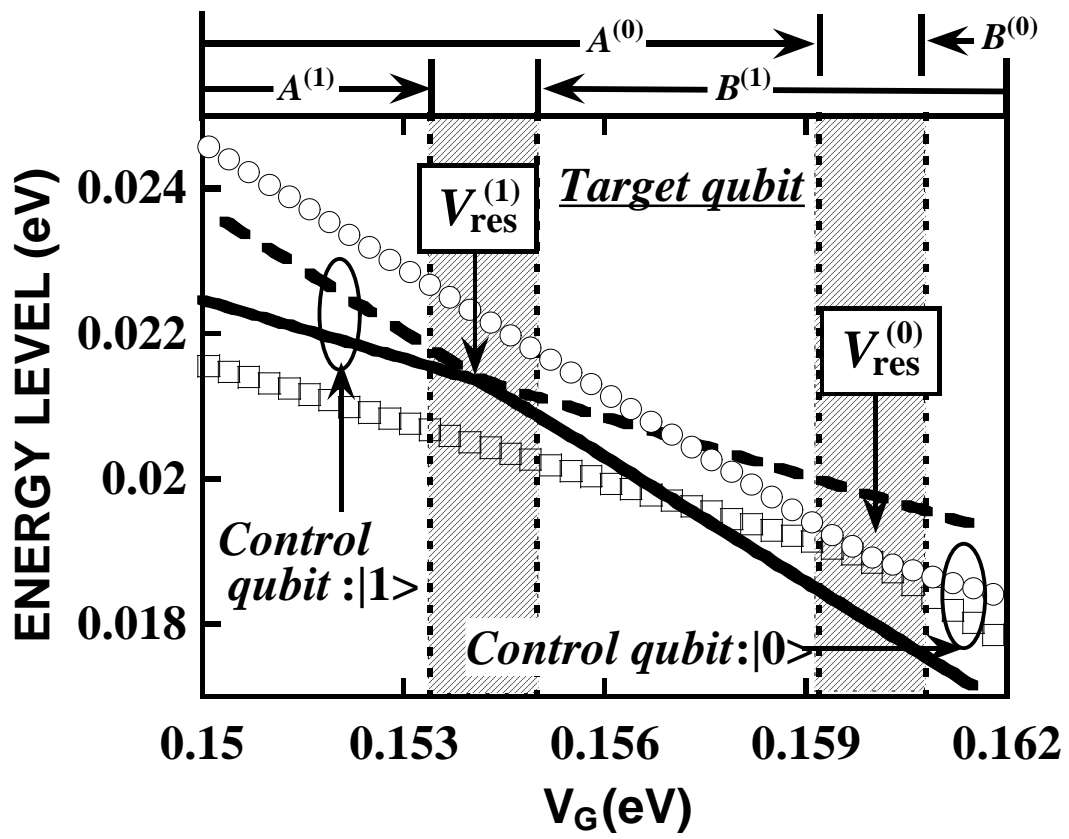


Fig.4: T. Tanamoto

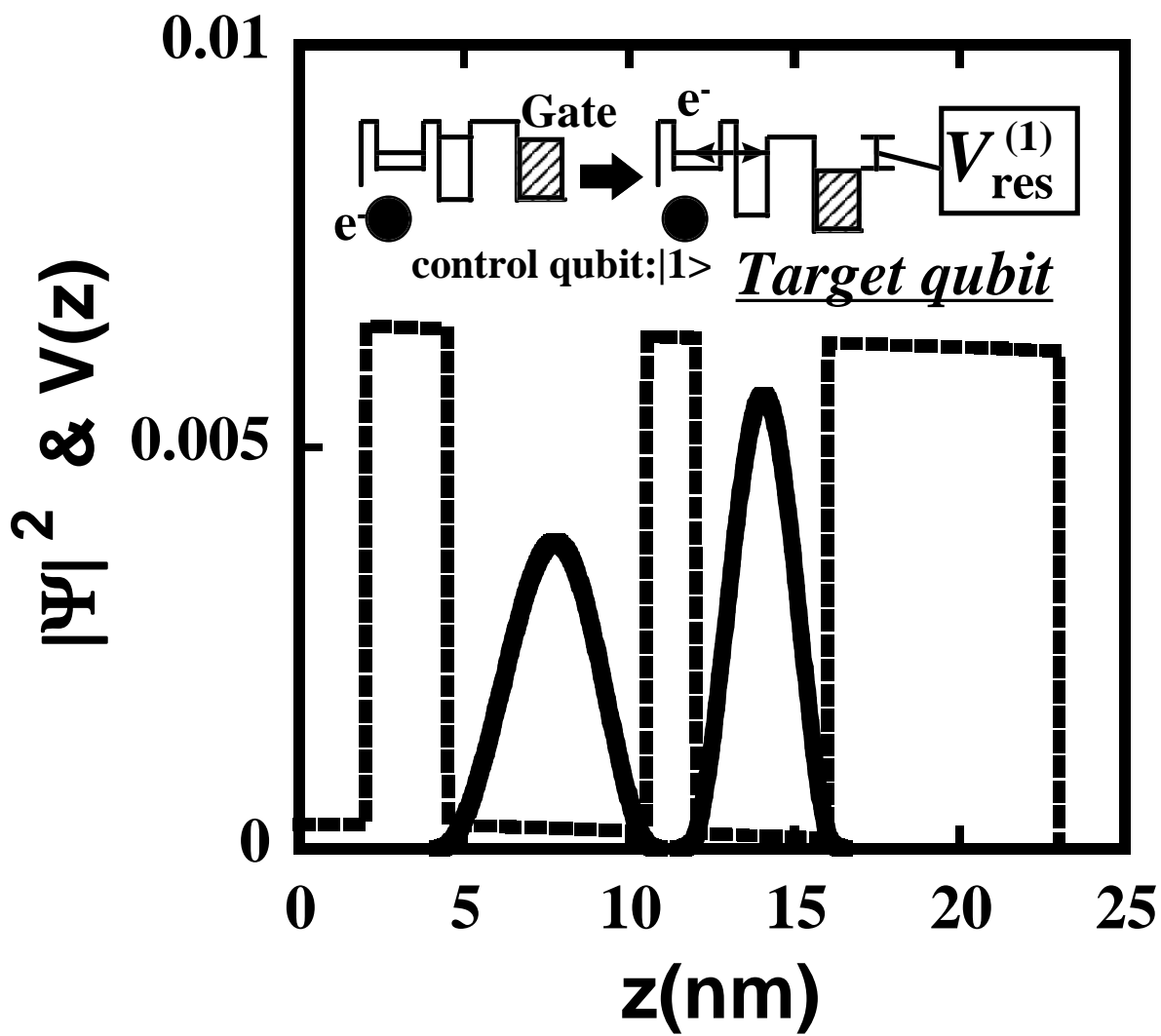


Fig. 5(a) : T. Tanamoto

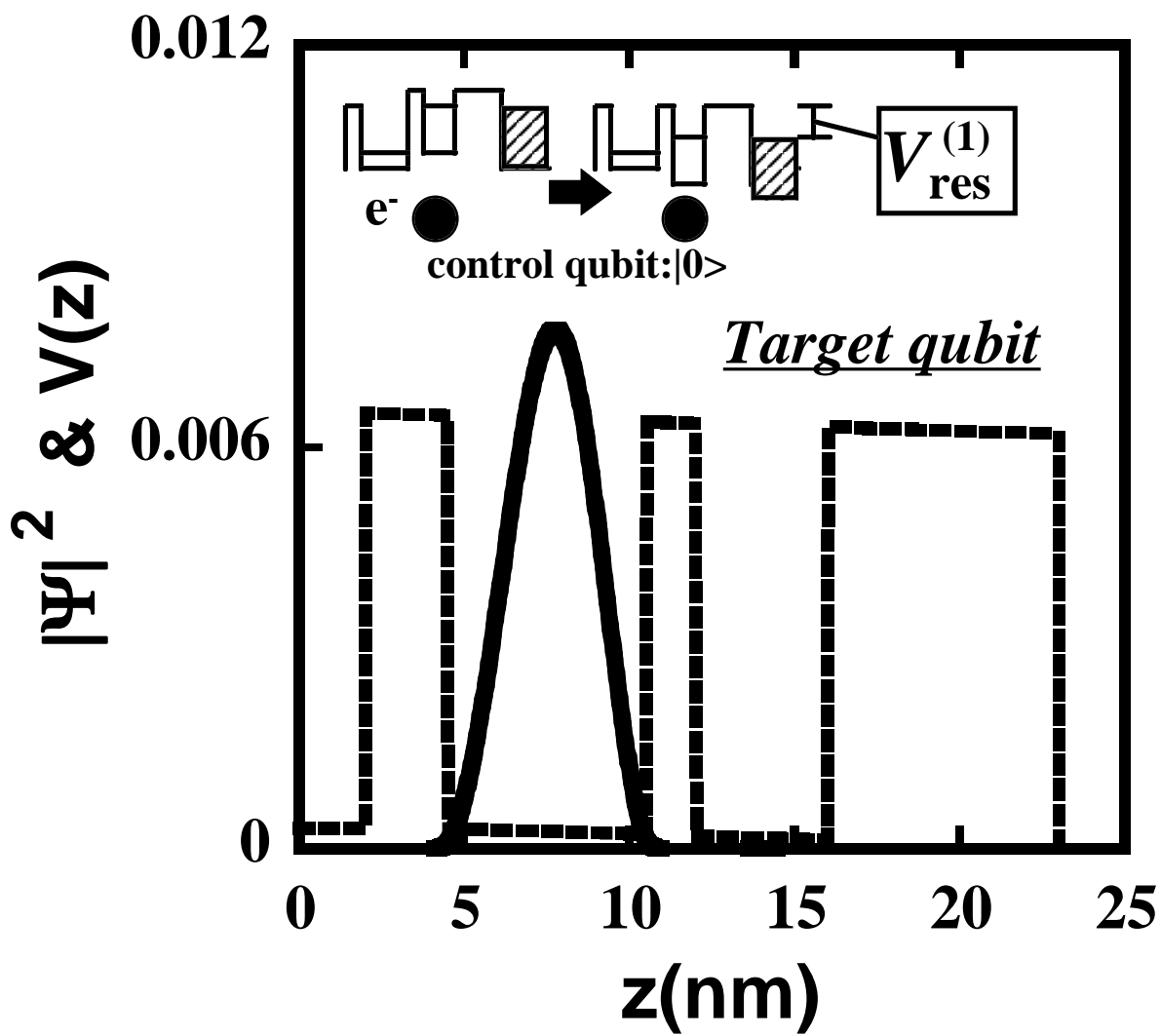


Fig. 5(b) : T. Tanamoto